

Bimetallic Castings in a Chromium–Nickel Stainless Steel Working Surface Layer Configuration with a Grey Cast Iron Base

Tomasz Wróbel · Jerzy Wiedermann ·
Piotr Skupień

Received: 3 September 2014 / Accepted: 11 November 2014 / Published online: 24 December 2014
© The Indian Institute of Metals - IIM 2014

Abstract The paper presents the problem of obtaining a permanent diffusion joint between the working surface layer and the base part in a bimetallic casting. The bimetallic castings studied here were obtained as a result of using the founding method of layer coating directly in the cast process, i.e., the so-called method of mould cavity preparation by monolithic insert. The castings prepared using this method consist of two fundamental parts, i.e., the base which constitutes typical foundry material, i.e., grey cast iron and the working surface layer which constitutes plate of chromium–nickel stainless steels, X2CrNi 18-9 and X2CrNiMoN22-5-3 grade. On the basis of the obtained results it was confirmed that the decisive phenomena that are needed to create a permanent joint between the two components of the bimetallic casting are carbon and heat transport in the direction from the high-carbon and hot base material which was poured into the mould in the form of liquid metal to the low-carbon and cold material of the working layer which was placed in the mould cavity in the form of a monolithic insert.

Keywords Bimetallic casting · Stainless steel · Cast iron · Diffusion · Microstructure

1 Introduction

The technology of bimetallic castings is gaining in importance, particularly when the criterion for highly usable properties concerns only the working surface layer and the rest of the casting is only a base part that is not exposed to the direct influence of factors causing abrasive or corrosion wear. This technology is the most economical way of enriching the surface of castings, as it allows for the production of layered elements directly in the cast process. Therefore, this technology can be significantly competitive for the commonly used technologies of surfacing by welding and thermal spraying because in addition to its economic advantages it does not generate opportunities for the development of cracks in the heat affected zone, which may arise as a result of making the layer by using the welding method.

In general, the technology of cast bimetallics containing a working layer and a base part is carried out based on two systems, i.e., liquid–liquid [1–4] and liquid–solid [5–23]. An example of the former is a technology in which two independent gating systems are made which guarantee a two-stage filling of the sand mould cavity. According to this manufacturing method the bimetallic elements of hammer [1, 2] or ball [3] mills are cast in material configurations of a resistant to abrasive wear chromium cast iron working layer with a ductile low-carbon cast steel base. The basis technology of bimetallic castings made in the liquid–solid system is the so-called method of mould cavity preparation. In this manufacturing method the element enriching the surface of the casting is placed in the mould in the form of a granular [5–8] or monolithic [9–23] insert directly before the molten metal is poured. Granular inserts are used to make bimetallic castings for the mining industry in material configurations with a hard working

T. Wróbel (✉)
Foundry Department, Silesian University of Technology,
Towarowa 7, 44-100 Gliwice, Poland
e-mail: tomasz.wrobel@polsl.pl

J. Wiedermann · P. Skupień
Institute for Ferrous Metallurgy, Karola Miarki 12-14,
44-100 Gliwice, Poland

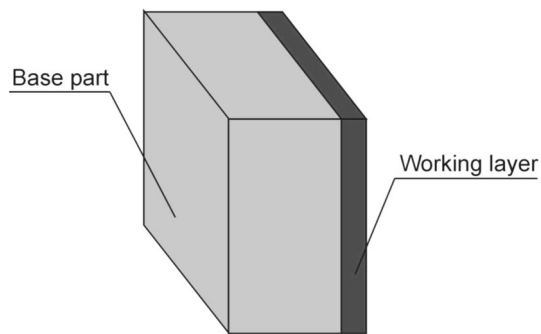


Fig. 1 Scheme of the bimetallic casting

surface layer of Fe–Cr–C [6, 7], Fe–Cr–C–Mo [5] or Ni–Cr–Fe–C [8] alloys with an unalloyed cast steel base. An example of technology using the monolithic insert are bimetallic castings in a configuration of chromium cast iron connected with the weldable low-carbon steel plate [9, 10]. However, a significant economic limitation of this manufacturing method is the need to preheat the steel plate (monolithic insert) that is placed in the mould. This treatment is carried out by two-stage mould pouring with the liquid cast iron. In the first stage the mould cavity beneath the steel plate is filled with a liquid metal for insert preheat. The layer of cast iron formed in this way is, after cleaning, separated from the casting. In the second stage the mould cavity over the steel plate is filled, in it the liquid metal forms a layer connecting with the plate and creating a bimetallic casting. However, the technologies of the bimetallic castings presented in the available literature have large limitations, e.g., decreased process economy due to the necessity of pouring two different alloys [1–4]

and a decrease in yield resulting from the necessity of applying insert preheating [9, 10, 12–17] and complication of the cast process by applying two gating systems [1–4, 9, 10].

Therefore, the aim of the paper is to describe a technology of bimetallic castings in a material configuration of chromium–nickel stainless steel–grey cast iron based on the liquid–solid method using a non-preheated monolithic insert. In the presented technology, preheating of the monolithic insert, which makes it easier to form a permanent joint between the working layer and the base part and also increases production costs as well as makes it difficult to place the steel plate in the mould cavity, was replaced by application of an activator covering the contact surface between both of the materials used.

2 Experimental Procedure

The study encompassed bimetallic castings which consisted of two fundamental parts, i.e., a base and a working surface layer (Fig. 1). The base part of the bimetallic casting was typical foundry material, i.e., grey cast iron with flake graphite, whereas the working layer was a plate of chromium–nickel stainless steels, i.e., austenitic X2CrNi 18-9 grade and ferritic–austenitic sort X2CrNiMoN22-5-3 grade. The chemical composition of the component materials of bimetallic castings used here are presented in Tables 1, 2, and 3.

For the test bimetallic castings with the ratio of thickness between the base and working part being 8:1 at 590,625 mm³ in volume, plates of the stainless steels were

Table 1 Chemical composition of the stainless steel X2CrNi 18-9 grade working layer of the bimetallic casting

Elements content (wt%)								
C	Cr	Ni	Si	Mn	Mo	P	S	Fe
0.030	19.200	9.800	0.900	1.450	0.200	0.030	0.002	Rest

Table 2 Chemical composition of the stainless steel X2CrNiMoN22-5-3 grade working layer of the bimetallic casting

Elements content (wt%)									
C	Cr	Ni	Si	Mn	Mo	P	S	N	Fe
0.020	22.500	6.200	0.300	1.010	3.100	0.020	0.001	0.150	Rest

Table 3 Chemical composition of the grey cast iron base part of the bimetallic casting with deviations containing all melts

Elements content (wt%)										
C	Mn	Si	Cr	Ni	Cu	Ti	V	P	S	Fe
3.10 ± 0.050	0.50 ± 0.050	1.70 ± 0.100	0.10 ± 0.020	0.05 ± 0.010	0.15 ± 0.030	0.01 ± 0.008	0.01 ± 0.005	0.12 ± 0.003	0.06 ± 0.010	Rest

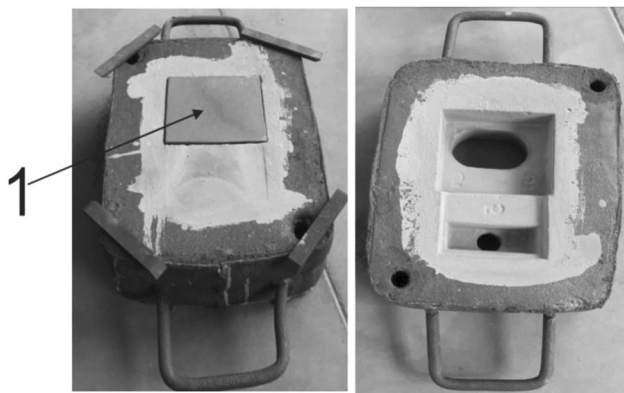


Fig. 2 View of the bottom part (*left*) and upper part (*right*) of a sand mould with a monolithic insert (*1*) placed in its cavity

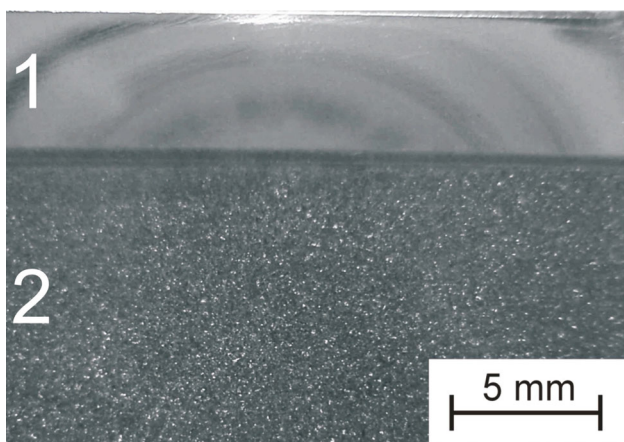


Fig. 3 Example a transverse section of the bimetallic casting: *1* working layer in the form of a stainless steel plate, and *2* the base part of grey cast iron

placed in sand moulds with no preheating (Fig. 2). These were then poured over with liquid cast iron in a pouring temperature of 1,450 °C. On the basis of results of previous studies [21], steel plates with a thickness of 5 mm were used. Their surfaces, remaining in direct contact with the liquid metal, were covered by an activator in the form of boron and sodium compounds, i.e., an aqueous solution of $\text{Na}_2\text{B}_4\text{O}_7 + \text{B}_2\text{O}_3$. These compounds promote the formation of a permanent joint between both materials of the layered casting by purification of the contact surface of the oxide layer, protection against the formation of a new oxide layer and by a decrease in the wetting angle on the insert, i.e., the liquid-metal boundary.

The quality of the joint in the bimetallic castings was evaluated on the basis of ultrasonic non-destructive testing done using the DIO 562 flaw detector by Starmans Elektronics. Then metallographic macro- and microscopic examinations were carried out. Metallographic samples etched in the reagent Mi19Fe contained: 3 g of ferric chloride, 10 cm³ hydrochloric acid and 90 cm³ ethanol. For structure research a light microscope (LOM) Nikon, scanning electron microscope (SEM) INSPECT F with microanalysis of the chemical composition (EDS) and a transmission electron microscope (TEM) FEI-Titan 80–300 kV were used. Moreover, in the procedure, TEM samples in the form of thin foils drawn from selected areas using a gallium ion gun, FEI-FIB Quanta 3D 200i, were used. Measurements of microhardness were done using an FM 700 Future-Tech (HV0,01). Numerical simulation of predicting the presence of phases in the microstructure based on the analysis done in ThermoCalc software and a computer simulation of the solidification of bimetallic

Fig. 4 Shape of the microstructure of a bimetallic casting in a configuration of the working layer in the form of a stainless steel X2CrNi 18-9 plate and the base part from grey cast iron

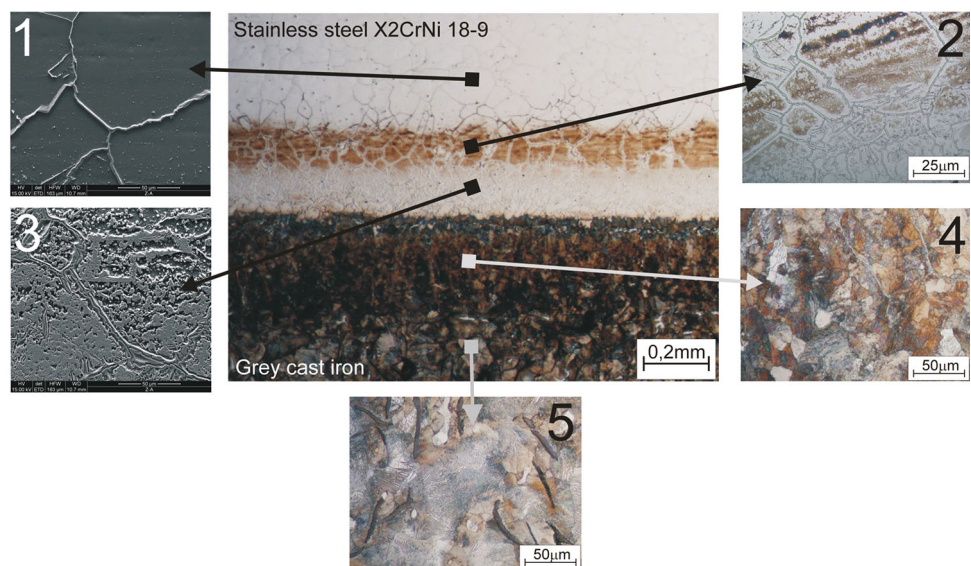


Fig. 5 Shape of the microstructure of a bimetallic casting in a configuration of the working layer in the form of a stainless steel X2CrNiMoN22-5-3 plate and the base part from grey cast iron

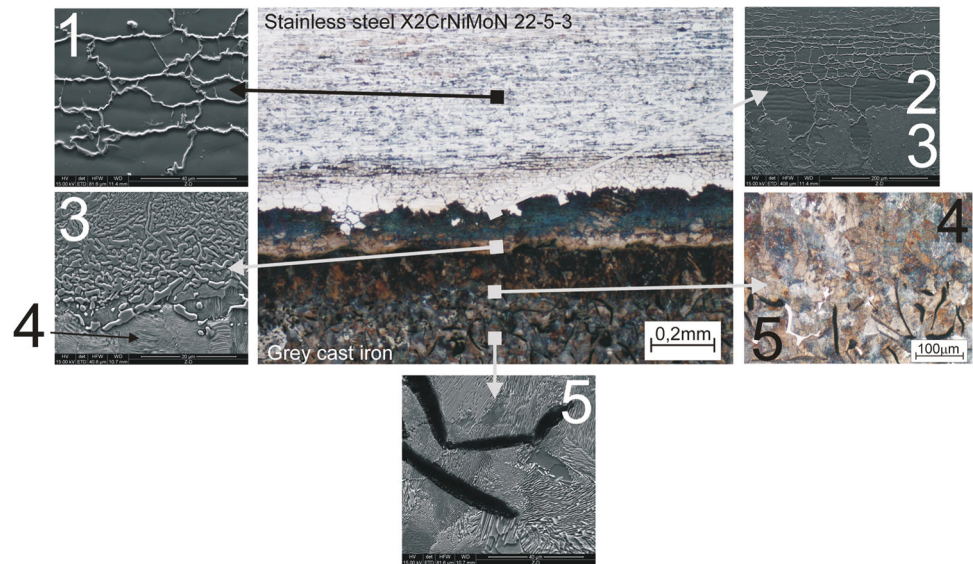
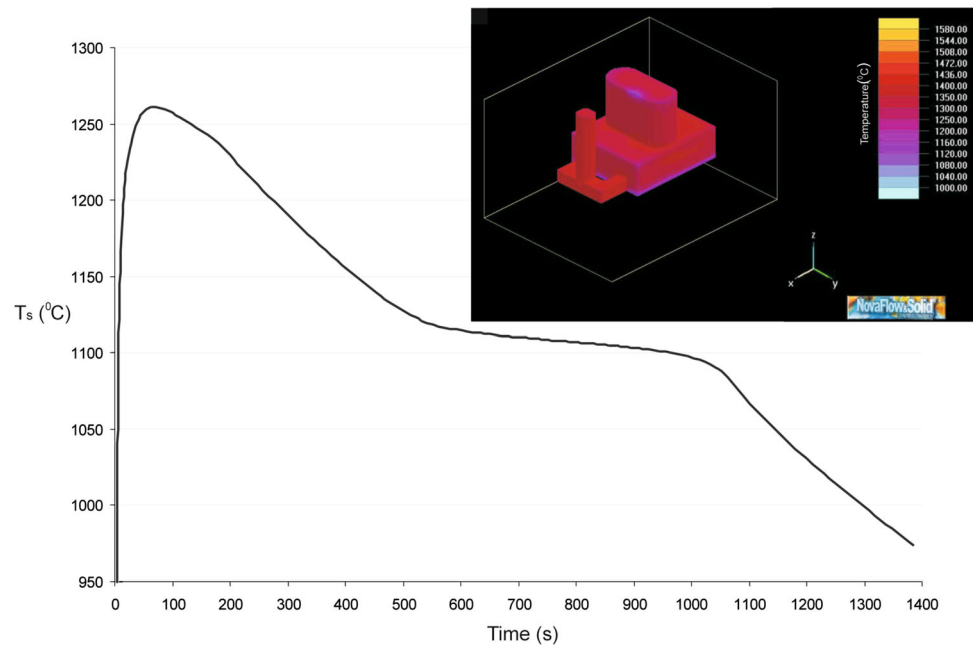


Fig. 6 Time characteristic of the contact temperature (T_s) on the boundary of a liquid metal (cast iron) and stainless steel X2CrNi 18-9 plate, determined on the basis of the results of a computer simulation of the solidification of a bimetallic casting made in NovaFlow&Solid software



casting using NovaFlow&Solid software were conducted for the assumed foundry technology.

3 Results and Discussion

Non-destructive ultrasonic testing showed that on the whole contact surface of both materials in the bimetallic castings a permanent joint was obtained, i.e., for which the bottom echo was larger than the echo of the transition zone (head placed on the side of the plate) between the working layer and the base part. These results were confirmed by a

macroscopic visual quality assessment conducted on selected sections of test bimetallic castings (Fig. 3).

Figures 4 and 5 present the microstructure of the obtained bimetallic castings. The joint obtained between the austenitic or ferritic–austenitic stainless steel and grey cast iron is durable and has a diffusion character. A decisive factor is carbon diffusion in the direction from the cast iron to the steel plate. The proximate result of this diffusion is the creation of transition zones which are structurally different from the cast iron and the steel plates used.

Moreover, the heating temperature of stainless steel has an effect on the formation of the transition zone's

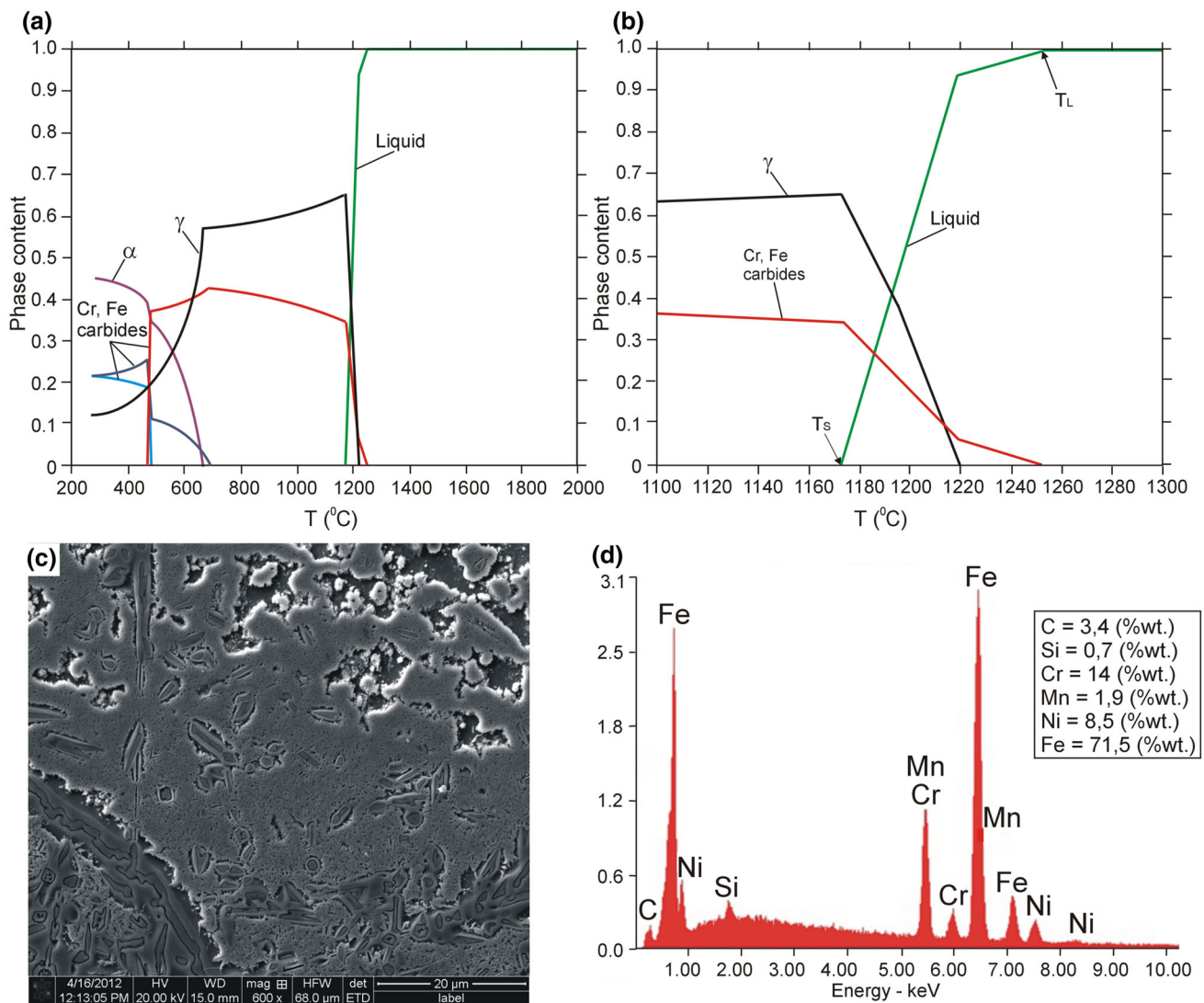


Fig. 7 Phase content in the function of temperature for zone 3 from Fig. 4, carried out in ThermoCalc software (a), a magnified fragment of the solidification range (b), microstructure of zone 3, SEM (c) and result of microanalysis of chemical composition EDS in zone 3 (d)

microstructure, and whose source is the liquid cast iron that was poured into the mould. For a pouring temperature of 1,450 °C of the cast iron and contact temperature T_s on the boundary of the liquid metal—the stainless steel plate is fixed on the basis of formulae [24]:

$$T_s = \frac{\sqrt{\lambda_n \cdot c_n \cdot \rho_n \cdot T_n} + \sqrt{\lambda_r \cdot c_r \cdot \rho_r \cdot T_r}}{\sqrt{\lambda_n \cdot c_n \cdot \rho_n} + \sqrt{\lambda_r \cdot c_r \cdot \rho_r}}, \quad (1)$$

where λ_n , λ_r are coefficient of thermal conductivity, suitable for liquid cast steel (base part of the bimetallic casting) and the steel plate (working layer of the bimetallic casting, W/(m K)), c_n , c_r are specific heat, suitable for the liquid cast steel (base part of the bimetallic casting) and the steel plate (working layer of the bimetallic casting, J/(kg K)), ρ_n , ρ_r are mass density, suitable for the liquid cast steel (base part of the bimetallic casting) and the steel plate

(working layer of the bimetallic casting, kg/m³), T_n is the temperature of liquid cast steel (base part of the bimetallic casting, °C), and T_r is the temperature of the steel plate (working layer of the bimetallic casting, °C), for the plate of stainless steel X2CrNi 18-9 grade is about 950 °C. After about 80 s from filling the mould with liquid metal, the contact temperature achieved maximal value is equal to about 1,260 °C, as the results of the computer simulation of solidification of the bimetallic casting show (Fig. 6). Whereas for the plate of stainless steel X2CrNiMoN22-5-3 grade the contact temperature is about 20 °C lower and is equal to 930 °C.

There are five zones present for the bimetallic casting in an X2CrNi 18-9 stainless steel working surface layer configuration with a grey cast iron base in the microstructure, as is shown in Fig. 4. The first and fifth zone

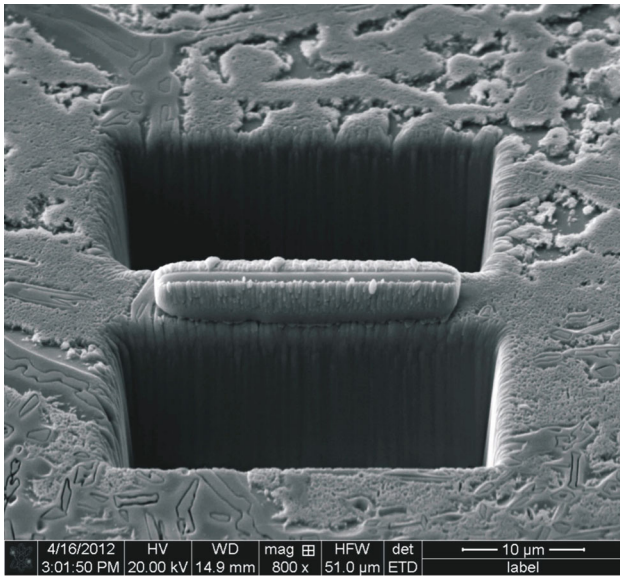


Fig. 8 Method of drawing thin foil from zone 3 from Fig. 4 to the TEM studies

have microstructures that are typical of alloys used adequately on the working layer and the base part of the bimetallic casting, i.e., austenite in zone one and flake graphite in the pearlite matrix in zone 5. The areas from 2 to 4 are transition zones. In zone 2, structural changes occurred in the solid state, i.e., as a result of carbonising connected with the diffusion of chromium induced by heating whose source was liquid cast iron poured into the mould, in this zone microstructures with carbides Cr_{23}C_6 in the γ (austenite) phase matrix were created. The result of the presence of carbides in zone 2 is an increase in microhardness from about 200 μHV in the austenitic zone 1 to 350 μHV and a decrease in corrosion resistance, as evidenced by the effects of microsection etching (pits), which clearly appear in the zone. Carbonising of zone 3, which is placed closer to the liquid cast iron poured into the mould than zone 2, decreases the liquidus temperature T_L to 1,250 °C and solidus T_S to 1,170 °C (Fig. 7).

As a result, zone 3 is melted by a high heating temperature which achieves a maximal value of about

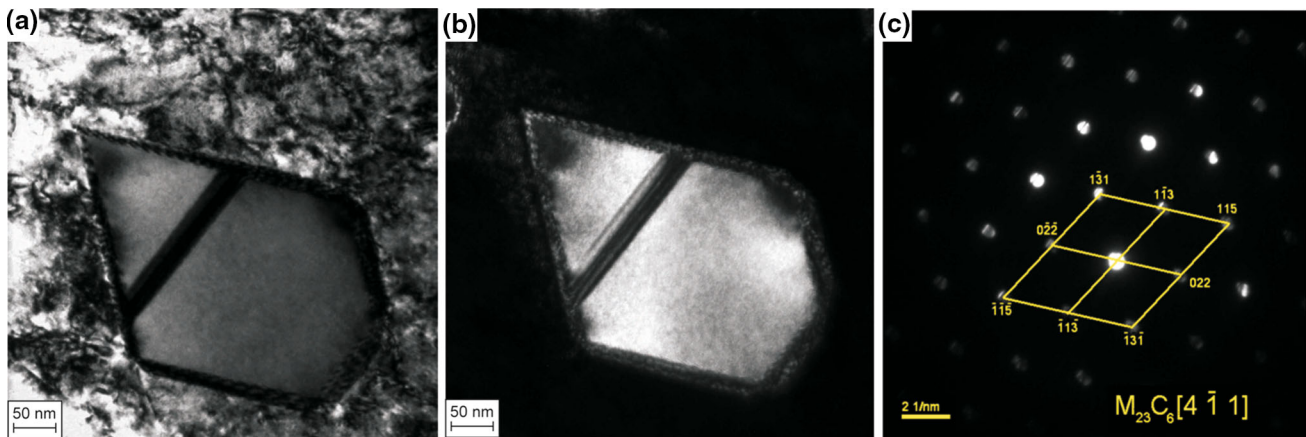


Fig. 9 $M_{23}C_6$ carbide in the microstructure of zone 3 from Fig. 4: **a** bright field, TEM, mag. $\times 43,000$, **b** dark field TEM, mag. $\times 43,000$ and **c** diffraction pattern from the area as in **a**

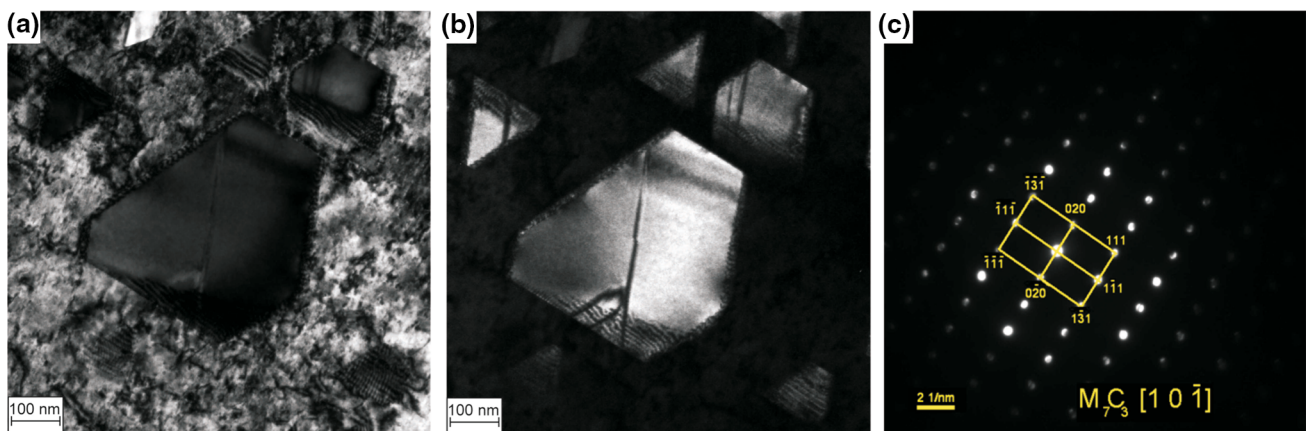


Fig. 10 M_7C_3 carbide in the microstructure of zone 3 from Fig. 4: **a** bright field, TEM, mag. $\times 27,000$, **b** dark field TEM, mag. $\times 27,000$ and **c** diffraction pattern from the area as in **a**

1,260 °C. Then zone 3 crystallises at a specified chemical composition, which decides about the microstructure containing Cr(Fe) carbides, mainly $M_{23}C_6$ and M_7C_3 grades in the $\alpha + \gamma$ (ferrite + austenite) matrix (Figs. 7, 8, 9, 10).

On the side of the base part is decarbonising zone 4. Depending on the local cooling rate and the chemical composition, in this zone a microstructure of pearlite is present with a microhardness of about 240 μ HV or a pearlitic–martensitic microstructure with a microhardness of about 350 μ HV (Fig. 11). Next, deep inside the base part a smooth transition takes place to high-carbon zone 5 containing flake graphite in the pearlite matrix.

There are also five zones in the bimetallic casting in an X2CrNiMoN22-5-3 stainless steel working surface layer configuration with a grey cast iron base in the microstructure, as shown in Fig. 5. As a result of the diffuse-thermal phenomenon occurring at the boundary of the steel plate–cast iron casting, the presence of the following zones in the microstructure of this bimetallic casting were confirmed:

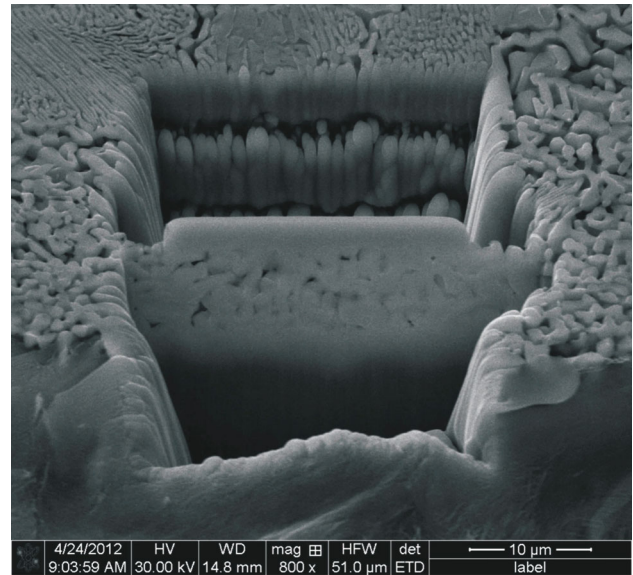


Fig. 13 Method of drawing thin foil from zone 3 from Fig. 5 to the TEM studies

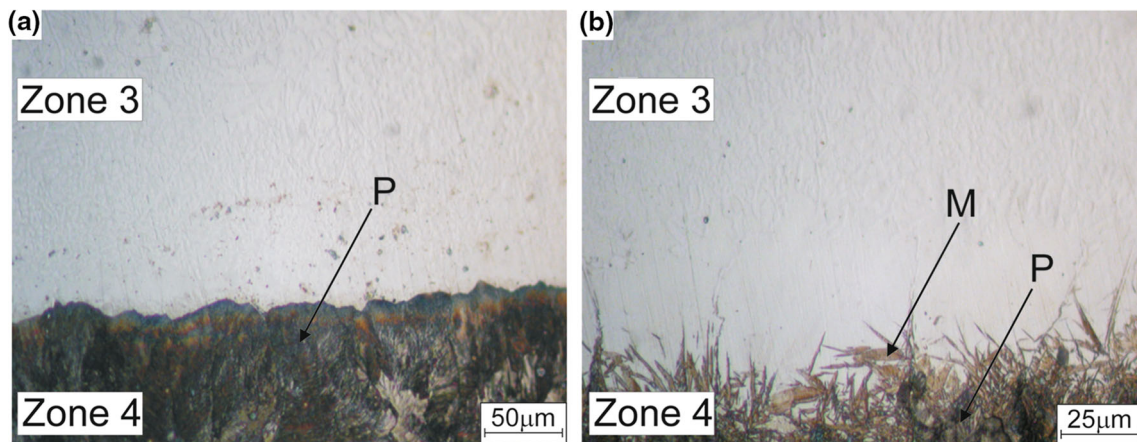


Fig. 11 Microstructure of the joint area between stainless steel X2CrNi 18-9 (zone 3) and grey cast iron (zone 4) on the boundary of the cast iron side are present: **a** pearlite (P) and **b** pearlite (P) and martensite (M), LOM, etching Mi19Fe

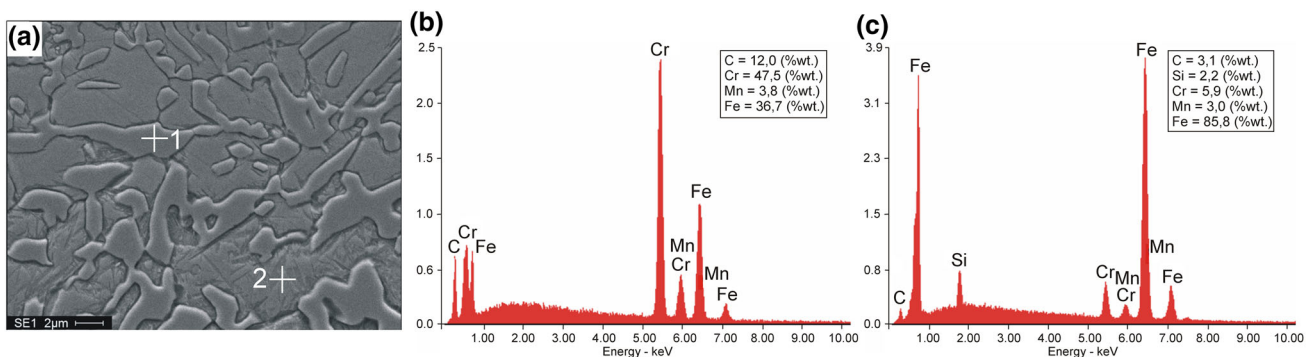


Fig. 12 Microanalysis of the chemical composition: **a** microstructure of the studied area in zone 3 from Fig. 5, SEM and **b** the result of EDS in point 1 (carbide) and **c** the result of EDS in point 2 (martensite matrix)

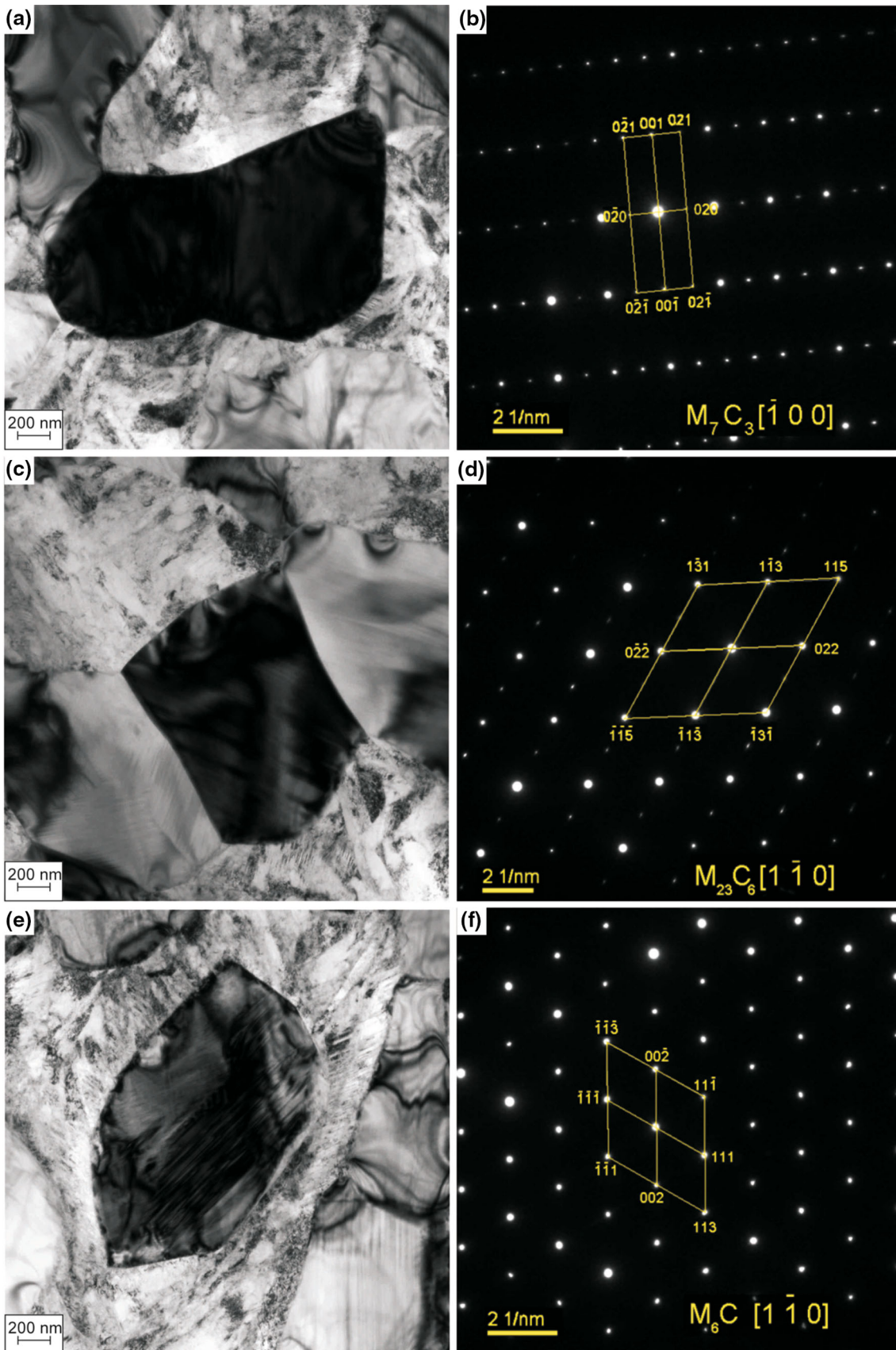


Fig. 14 Carbides in the microstructure of zone 3 from Fig. 5: **a** M_7C_3 : bright field, TEM, mag. $\times 10,000$, **b** diffraction pattern from the area as in **a**, **c** $M_{23}C_6$: bright field, TEM, mag. $\times 10,000$, **d** diffraction pattern from the area as in **c**, **e** M_6C : bright field, TEM, mag. $\times 10,000$ and **f** diffraction pattern from the area as in **e**

Zone 1: Ferritic–austenitic ($\alpha + \gamma$), i.e., proper for the working layer of stainless steel X2CrNiMoN22-5-3 grade.

Zone 2: Containing coarse-grained austenite resulting from, on the one hand, heating of this zone by the liquid cast iron poured into the mould to a temperature of $\alpha + \gamma$ phase stability which, in connection with the subsequent slow cooling of the casting allows to increase the amount of austenite by phase change $\alpha \rightarrow \gamma$. On the other hand, stabilisation of the austenitic microstructure without ferrite favours carbonising of this zone by contact of the steel plate with the liquid cast iron. This carbonising contributes to a significant increase in the amount of the nickel equivalent, whose stabilising phase γ is:

$$Ni_{eq} = Ni\%_{mas.} + 30(C\%_{mas.} + N\%_{mas.}) + 0.5Mn\%_{mas.}, \quad (2)$$

which simultaneously does not affect the amount of the chromium equivalent, whose stabilising phase α is:

$$Cr_{eq} = Cr\%_{mas.} + Mo\%_{mas.} + 1.5(Si\%_{mas.} + Nb\%_{mas.}). \quad (3)$$

Zone 3: Created from the liquid phase on the one hand as a result of carbonising, which decreases both the liquidus and solidus temperature and, on the other hand, as a result of the high heating temperature of this border zone by liquid cast iron poured into the mould. The chemical composition of zone 3 decides about its microstructure which contains a high amount of Cr(Fe) carbides, mainly $M_{23}C_6$, M_7C_3 and M_6C grades in the martensite matrix (Figs. 12, 13, 14). This zone's microhardness is about 900 μ HV.

Zone 4: The decarbonising zone of the base part of the bimetallic casting contains pearlite.

Zone 5: Flake graphite in the pearlite matrix, i.e., proper for the base part of grey cast iron.

4 Summary

On the basis of the obtained results we could confirm that decisive phenomena needed create to a permanent joint between the two components of the bimetallic casting, i.e.,

X2CrNi 18-9 or X2CrNiMoN22-5-3 stainless steels and grey cast iron, are carbon and heat transport in the direction from the high-carbon, hot material of the base part, which was poured into the mould in the form of liquid metal to low-carbon, cold material of the working layer, which was placed in the mould cavity in the form of a 5 mm thick monolithic insert. The decisive influence of carbon on forming the joint between the working layer and the base part results from this element's easiness in transport with the interstitial mechanism from one material to another, as distinguished from Fe, Cr or Ni transport with the vacancy mechanism. Therefore, as a result of this phenomena in the microstructure of bimetallic casting three transition zones were created which were situated between the microstructure proper for the working layer, i.e., austenitic for stainless steel X2CrNi 18-9 grade or ferritic–austenitic for stainless steel X2CrNiMoN22-5-3 grade and the microstructure proper for the base part, i.e., flake graphite in the pearlite matrix. On the side of the base part of the bimetallic casting is the first transition zone containing pearlite without graphite, which was created as a result of decarbonising connected with carbon transport in the direction to this element's lower concentration, i.e., to the working layer. Then there is the transition zone created from the liquid phase as a result of carbonising which decreases both the liquidus and solidus temperature in this border area of the steel plate and next melts under the influence of high temperature resulting from heat transport in the direction from the liquid cast iron to the monolithic insert. The chemical composition obtained in this zone determines the crystallisation of the microstructure consisting of carbides, mainly Cr and Fe, in the solid solution matrix. On the side of the working layer the transition zone created in the solid phase is present as a result of carbonising (insufficient to significantly reduce the melting point) and cooling from a high temperature (insufficient to melt this area). This zone, depending on the stainless steel used, contains Cr carbides in the austenitic matrix (steel X2CrNi 18-9) or coarse-grained austenite (steel X2CrNiMoN22-5-3).

To sum up, bimetallic castings made in the stainless steel–grey cast iron configuration allow to obtain technologically useful bimetals, both for the sake of high quality of the joint and high useful properties of the working layer.

Acknowledgments The financial support from the Polish National Science Centre is kindly acknowledged.

References

1. Žic S, Džambas I, and Konić M, *Metallurgija* **48** (2009) 51.
2. Hua W, *Adv Mater Res* **535-537** (2012) 266.
3. Xiaofeng X, Shengping Y, Xiaoguang Z, and Qiong X, *China Foundry* **9** (2012) 136.

4. Marukovich E, Branovitsky A, Na Y, Lee J, and Choi K, *Mater Des* **27** (2006) 1016.
5. Heijkoop T, and Sare I, *Cast Met* **2** (1989) 160.
6. Gawroński J, Szajnar J, and Wróbel P, *J Mater Process Technol* **157–158** (2004) 679.
7. Szajnar J, Wróbel P, and Wróbel T, *Arch Foundry Eng* **8** (2008) 105.
8. Wróbel T, in Proc *METAL 2011 20th Anniversary International Conference on Metallurgy and Materials*, (eds) Podjuklová J and Štěpánek I, Tanager, Brno (2011), p 758.
9. Jura S, and Suchoń J, *Solidif Met Alloys* **24** (1995) 67 (in Polish).
10. Bartocha D, Suchoń J, and Jura S, *Solidif Met Alloys* **38** (1998) 151 (in Polish).
11. Qian M, Harada S, Kuroshima Y, and Nagayoshi H, *Mater Sci Eng A* **A208** (1996) 88.
12. Arnold B, Heijkoop T, Lloyd P, Rubens G, and Sare I, *Wear* **203–204** (1997) 663.
13. Kilarski J, and Suchoń J, *Arch Foundry* **6** (2006) 266.
14. Şimşir M, Kumruoğlu L, and Özer A, *Mater Des* **30** (2009) 264.
15. Cingi C, Rauta V, Niani E, and Orkas J, *Mater Sci Forum* **654–656** (2010) 2712.
16. Xiong B, Cai C, and Lu B, *J Alloy Compd* **509** (2011) 6700.
17. Xiong B, Cai C, Wan H, and Lu B, *Mater Des* **32** (2011) 2978.
18. Viala J, Peronnet M, Barbeau F, Bosselet F, and Bouix J, *Composites A* **33** (2002) 1417.
19. Szymczak T, *Arch Foundry Eng* **11** (2011) 215.
20. Lucey T, Wuhler R, Moran K, Reid M, Huggett P, and Cortie M, *J Mater Process Technol* **212** (2012) 2349.
21. Cholewa M, Wróbel T, Tenerowicz S, and Szuter T, *Arch Metall Mater* **55** (2010) 771.
22. Wróbel T, Cholewa M, and Tenerowicz S, *Arch Foundry Eng* **11** (2011) 105.
23. Wróbel T, *J Mater Eng Perform* **23** (2014) 1711.
24. Duda P, and Taler J, *Solving Direct and Inverse Heat Conduction Problems*, Springer, Berlin (2006), p 363.